WARSAW UNIVERSITY OF TECHNOLOGY Index 351733
FACULTY OF CIVIL ENGINEERING
COMMITTEE FOR CIVIL AND WATER ENGINEERING
POLISH ACADEMY OF SCIENCES ISSN 1230-2945

DOI: 10.24425/ace.2023.145284

ARCHIVES OF CIVIL ENGINEERING

Vol. LXIX ISSUE 2 2023

pp. 551 –569

Research paper

Evaluation of the influence of the glass fiber mesh on the deflection basin parameters of a flexible pavement located in the area of mining activity

Mateusz Kałuża[1], Mirosław Kotasiński[2], Joanna Bzówka[3]

Abstract: Rehabilitation treatments applied to a local road prone to terrain subsidence from mining excavation should be designed considering cost-efficient and effective reinforcement solutions. In the analysed case, a glass-fibre mesh was applied under asphalt concrete layers in 2008, in one lane while another was left without the reinforcement. The main objective of this paper was to investigate the effectiveness of reinforcement by analysing the amount of produced on the pavement and the influence on pavement deflection. It was found that the reinforcement retracted the number of cracks, however, did not affect the bearing capacity. The influence of the applied geosynthetic was manifested in the values of the radius of curvature. The overall technical state of the road requires immediate treatment and the applied reinforcement proved obsolete because in this particular case of road located in the mining active terrain the glass fiber mesh did not prolong the life of the pavement.

Keywords: glass fiber mesh, mining subsidence, pavement reinforcement, terrain subsidence, FWD, deflection basin parameters

[1]MSc., Eng., Silesian University of Technology, Faculty of Civil Engineering, Akademicka 5, 44-100 Gliwice, Poland, e-mail: mateusz.kaluza@polsl.pl, ORCID: 0000-0002-9761-9066
[2]PhD., Eng., Silesian University of Technology, Faculty of Civil Engineering, Akademicka 5, 44-100 Gliwice, Poland, e-mail: miroslaw.kotasinski@polsl.pl, ORCID: 0000-0002-5588-0741
[3]PhD., Eng., Silesian University of Technology, Faculty of Civil Engineering, Akademicka 5, 44-100 Gliwice, Poland, e-mail: joanna.bzowka@polsl.pl, ORCID: 0000-0002-1765-7354

1. Introduction

District and municipal roads represent more than 87% of all roads in Poland, in addition to the voivodeship and national roads. Proper allocation of public money between rehabilitation treatment and a full rebuild of construction is a common dilemma among road managements, who seek newer solutions to prolong fatigue resistance and cost efficiency of rehabilitation treatments. The problem with pavement fatigue resistance intensifies when a designed structure is located in an area prone to terrain subsidence that occurs when underground mineral deposits, for example, coal, are extracted [1, 2]. The road analysed in this article lies in the mining subsidence area in Upper Silesia in Poland, where coal mining has led to ground deformation since the very beginning of the mining industry in the XIX century. The void in the rock massif after the coal excavation collapses over time and leads to the subsidence of the terrain. Deformations are divided into linear and non-linear [2]. The first one is the typical subsidence shown in Fig. 1 and characterised by the mining terrain categories shown in Tab. 1 while the latter are irregular and extremely hard to predict, often manifesting as cavities, ground collapse, and other local ground surface disruptions [3, 4].

Non-linear deformations are more common in shallow mining with shaft depths less than 100 m. Linear deformations can be predicted and characterised with the following parameters:

- Subsidence w [m],
- Inclination T [mm·m^{-1}],
- The radius of curvature R [km],
- Horizontal displacement u [m],
- Horizontal strain ε [mm·m^{-1}].

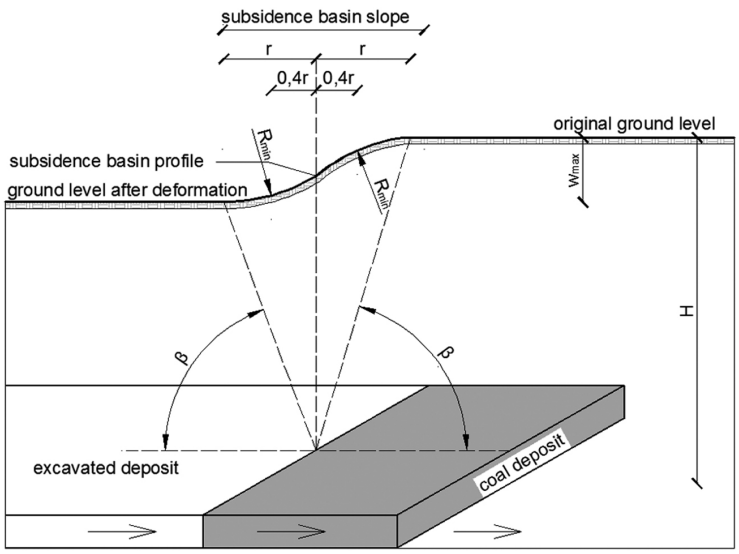

Fig. 1. Mining subsidence mechanism

Polish classification of mining areas shown in Table 1 consists of 6 categories, where 0 represents the lowest when no mining influence occurs and V is the highest, where localisation of any structure should be avoided. The terrain is counted into a specified category by the highest value of the parameters shown below. Inclination and radius of curvature describe the deformation that indicates problems with holding the construction elements together (e.g., bridges and pylons). Horizontal strain and displacement are a measure of ground weakening due to unloose movements between grains [4]. Total subsidence is crucial for roads, pipelines, or sewer systems where designed profiles and elevations are essential for proper functionality [5, 8]]. The increase in terrain deformations and their maximal values depends heavily on the speed of exploitation, fast leading to a reduction in the maximum strain values but increasing the increment and slow leading to a lower increment but higher total value of subsidence [9].

Table 1. Polish categories of mining terrains [9]

Category	Inclination T [mm·m^{-1}]	Radius of curvature R [km]	Horizontal strain ε [mm·m^{-1}]
0	$T \leq 0.5$	$40 \leq \lvert R\rvert$	$\lvert\varepsilon\rvert \leq 0.3$
I	$0.5 < T \leq 2.5$	$20 \leq R < \lvert 40\rvert$	$0.3 < \lvert\varepsilon\rvert \leq 1.5$
II	$2.5 < T \leq 5$	$12 \leq R < \lvert 20\rvert$	$1.5 < \lvert\varepsilon\rvert \leq 3$
III	$5 < T \leq 10$	$6 \leq R < \lvert 12\rvert$	$3 < \lvert\varepsilon\rvert \leq 6$
IV	$10 < T \leq 15$	$4 \leq R < \lvert 6\rvert$	$6 < \lvert\varepsilon\rvert \leq 9$
V	$15 < T$	$R < \lvert 4\rvert$	$9 < \lvert\varepsilon\rvert$

Rigid pavements, due to their high stiffness modulus, are prone to permanent deformation and damage, and therefore in mining subsidence areas, flexible pavements are the only viable option. Changes in the stress state in the subgrade lead to a critical bearing capacity. Because the maximum bearing capacity of pavement construction is bounded by the subgrade bearing capacity, it decreases accordingly. An additional factor that reduces the bearing capacity of pavement construction is the changing and unstable levels of groundwater that often accompany mining exploitation. The main problem is that horizontal unloosing deformations cause tensile stress in the structure and between the construction layers, subgrade/subbase [7, 13]. This additional tensile stress can also cause the loss of integrity of the aggregate base course. Additional tensile stress in the upper layers of pavement construction, especially when the temperature is low, can lead to intense cracking propagation. The influence of mining subsidence is hazardous for the durability and safety of pavement construction, leading to a problem of finding a proper solution to protect pavement construction from mining subsidence but also from typical distresses, which applies to both new and rehabilitated roads. The analyzed section of pavement was rehabilitated in 2008 by milling the existing asphalt layers and applying new ones $-3 \div 6$ cm of levelling course, 6 cm of binder course and 4 cm of surface course. The right lane was reinforced with a fibre-glass mesh (breaking strength 50/50 kN/m at breaking elongation 3%) applied

on the existing construction under the base course while the left lane was left without reinforcement. The existing structure was shown in Fig. 3, together with the test sections. It lies in the mining area of the 1st category and the measured total subsidence from 2008 to 2019 was around 20 cm accordingly with Fig. 2. Ten years after rehabilitation treatments author decided to investigate the effectiveness of the applied solutions, having in mind the continuous mining subsidence influence. The main objective of this paper is to identify the impact of applied reinforcement on the fatigue resistance of the pavement under the influence of mining activity.

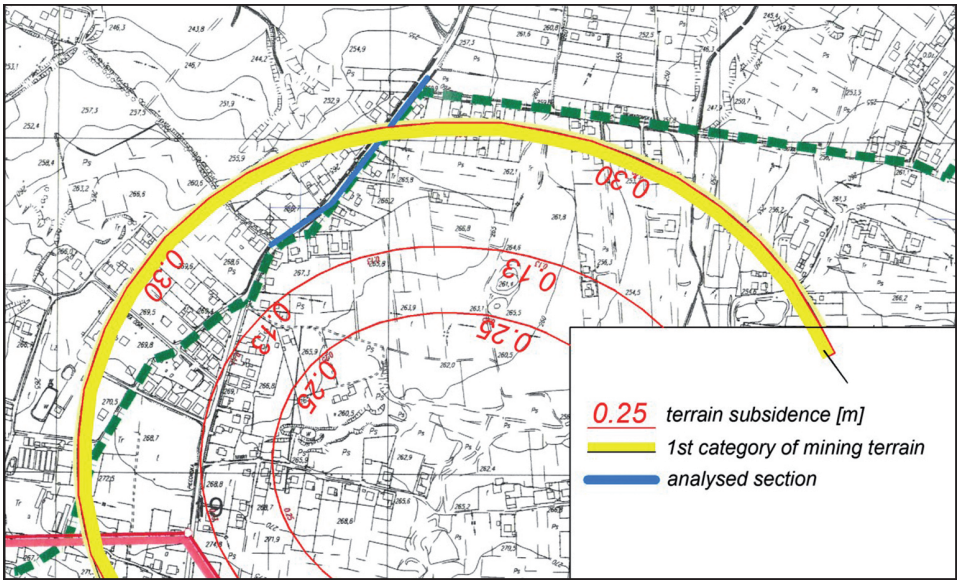

Fig. 2. Map of the subsidence of the terrain due to a mining excavation from 2009 to 2019. The blue line shows the analyzed section

The use of the geosynthetic layer as a subgrade reinforcement under mining influences in flexible pavement construction has been widely described. It was found to be effective in stabilising the embankment and preventing changes in the stiffness of the pavement layers due to mining exploitation [7]. The appropriate application allowed to build and maintain the A1 motorway in heavy mining [11, 12]. For a proper reinforcement effect, the geosynthetic should be located in the tension zone as low as possible and a proper bond between the geogrid and the asphalt layers should be provided [14]. With the proper type of geosynthetic, the stiffness and bearing capacity of the asphalt layers is increased; interlocking with asphalt concrete contributes to the restraining effect [15, 16]. The application directly on top of the old asphalt layer under the overlay allows delay or prevent propagation of cracks between layers and increases the rutting resistance [17]. Case studies conducted on heavy-traffic highways have shown that the fatigue life of glass fiber mesh reinforced pavement may be prolonged even by 6 years compared to unreinforced construction [18]. Laboratory tests

confirmed an increase in the fatigue resistance of reinforced pavement samples [19, 20]. The increase of pavement fatigue resistance was proven. Reinforcement applied under or in asphalt layers has the following functions:

- stress-relief,
- improvement of the fatigue resistance of the asphalt concrete layer,
- improves shear resistance to rutting in high-stress locations,
- delay of crack propagation.

Among the previously mentioned functions of the geosynthetic, the most effective are those applied to subgrades and embankments for new and rehabilitated roads [7, 10]. The application below the subbase allows to reduce the influence of horizontal unloosing strains and thus to improve a whole pavement construction's resistance to loss of the equilibrium state from mining subsidence [11]. The solution mentioned solution does not completely prevent subsidence but can decrease them significantly [7, 13]. Some doubts arise as the trend to apply interlayer reinforcement in pavement construction grows. The popularity of this solution amongst road management units comes from the assumption that the application of reinforcement just under asphalt layers will always increase the pavement fatigue resistance. This approach is typical for all types of roads but may prove problematic when used for roads that have not been adequately designed to withstand mining influences. Proper form of geosynthetic reinforcement is still a matter of contention despite years of practical experience and research, especially when terrain subsidence is considered. Mining subsidence is still an up-to-date problem that is present in all places around the world where the mining industry actively operates.

2. Research methods

The research was carried out in two stages, starting with the condition of the evaluation of the surface using a non-destructive visual method developed by the General Directorate of National Roads and Highways [21, 22]. The entire system for the evaluation of the pavement surface consists of the following types of data: bearing capacity, crack state, roughness index for a longitudinal profile, rutting, and frictional properties. In the analyzes performed, the cracking state was determined as it describes a loss of integrity of the pavement surface.

A reliable indicator of surface cracking describes a state of cracking based on the visual inventory of the following pavement surface distresses: fatigue, transverse and longitudinal crackings, potholes, patching, polished aggregate, and ravelling. After measurements, surface distresses were categorised by the degree of severity into two groups, high severity crackings (unsealed and wide-open with crumbled and cracked edges) and low severity crackings (sealed and narrow or unsealed but without crumbled edges). In the areas of high severity fatigue crackings, no additional crackings were counted while in the areas of low severity fatigue crackings additional distresses were counted as with the small severity. In the next step, the reliable state of the cracking indicators was calculated following that longitudinal and transverse crackings were summed up as linear crackings as in the

Equation (2.1).

$$P_{ij} = a \cdot \left(\frac{X}{b}\right)^{c} \cdot f \tag{2.1}$$

where: P_{ij} – points signed to distress i with severity j, where j is omitted when severity is not distinguished, X – distress amount – length for linear crackings and area for fatigue cracking, a, b, c – assigned parameters determined empirically in the guide, f – traffic load coefficient.

The number of points to evaluate the particular type of distress when severity is distinguished is calculated from the following equation.

$$P_i = 0.9 \cdot P_{ij\,\max} + 0.1 \cdot \sum_j P_{ij} \tag{2.2}$$

where: P_i – points signed to distress i, P_{ij} – points signed to distress i with severity j, j max – severity with the highest number of points assigned.

The equivalent index for linear and fatigue crackings P is then calculated as shown in Eq. (2.3):

$$P = 0.9 \cdot P_{i\,\max} + 0.1 \cdot \sum P_i \tag{2.3}$$

where: P – equivalent points index for linear and fatigue crackings, i max – distresses with the highest number of assigned points.

The state of the cracking indicator n_m is then expressed with precision to two decimal places, according to the Eq. (2.4):

$$n_m = \max\left(1 - \frac{P}{100},\ 0\right) \tag{2.4}$$

Calculated values should be in the range of 0 to 1 where a lower indicator value results in a higher amount of distress. The primary purpose of the stage was to determine the influence of interlayer reinforcement on the frequency of distress occurrence. The second step consisted of pavement deflection analyses with a focus on a calculated value of reliable deflection and a mean value of standardised deflection. Measurements were taken with a falling weight deflectometer in a trace of a right wheel every 25 m for each lane – reinforced and unreinforced. Measurements were performed in 2019 and 2021; the second measurement was performed as close to the previous test spots as possible, considering traffic and safety reasons. Differences between the locations of testing points may generate initial inaccuracies but do not significantly change the analyses presented. The temperature in the middle height of the asphalt layer was 28°C during the first measurement in 2019 and 22°C during the measures taken in 2021. The calculated deflections were adjusted to a temperature of 20°C and a load of 50 kN and compared with the allowed value of deflection for this class of roads. Equations (2.5) to (2.7) represent the procedure to determine the value of reliable deflection U.

$$U = \frac{\sum_{i=1}^{n} us_i}{n} + Dus \tag{2.5}$$

$$us = D_0 \cdot \frac{50}{F} \cdot f_t \cdot f_s \cdot f_p \tag{2.6}$$

$$f_T = 1 + 0.02(20 - T) \tag{2.7}$$

$$us' = D_0 \cdot \frac{50}{F} \cdot f_t \tag{2.8}$$

where: U – reliable pavement deflection [µm], us – standardised deflection [µm], n – the number of standardised deflections in the analysed section [–], f_T – correction coefficient converting the deflection values to the standard temperature of 20°C [–] Eq. (2.7), f_S – season coefficient, for August $f_s = 1.17$, for November $f_S = 1.25$, f_P – base coefficient, for flexible pavement $f_p = 1.0$, Dus – standard deviation of standardised deflections for analysed section of pavement, us' – standardised deflection without f_s and f_p corrections [µm].

The results were compared between lanes and sections (Fig. 3) to determine the influence of the applied glass fiber mesh on the deflection value. The final step of the analysis was to determine the following deflection bowl parameters:

– *BLI* (Base Layer Index also called Surface Curvature Index SCI) – characterizes the condition of the pavement layers

$$BLI = D_0 - D_{300} \tag{2.9}$$

where: D_0 – maximum deflection [µm], D_{300} – deflection measured with load cell at the distance 300 mm [µm].

– *MLI* (Middle Layer Index also called Base Damage Index) – characterizes the condition of the base layer

$$MLI = D_{300} - D_{600} \tag{2.10}$$

where: D_{300} – deflection measured with load cell at the distance 300 mm [µm], D_{600} – deflection measured with the load cell at a distance of 600 mm [µm].

– *LLI* (Lower Layer Index, also called Base Curvature Index) characterizes the condition of the subgrade

$$LLI = D_{600} - D_{900} \tag{2.11}$$

where: D_{600} – deflection measured with the load cell at a distance of 600 mm [µm], D_{900} – deflection measured with load cell at the distance 900 mm [µm].

– *RoC* (Radius of Curvature) – characterizes the condition of the pavement layer and base layer:

$$RoC = \frac{L^2}{2D_0\left(1 - \frac{D_{200}}{D_0}\right)} \tag{2.12}$$

where: $L = 200$ mm for the FWD, D_{200} – deflection measured with the load cell at the distance of 200 mm [µm], D_0 – maximum deflection [µm].

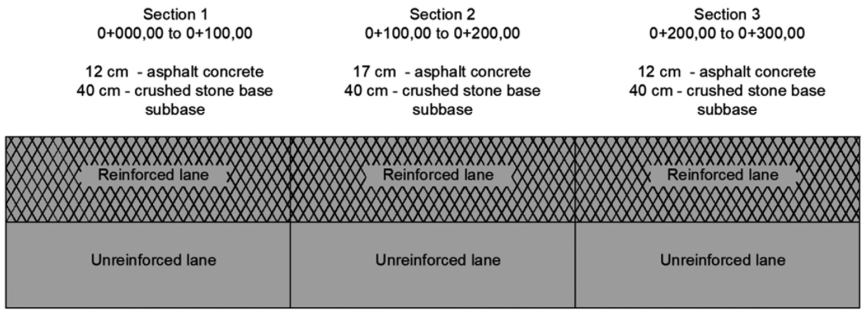

Fig. 3. Test sections with pavement construction

3. Results

After analysing the reliable state of cracking indicators shown in Figure 4, it was noticed that a road lane reinforced with glass-fibre mesh is classified into B-category – sufficient condition on each section of the lane according to Table 2. The unreinforced lane also qualifies into category B, except for the second section, which qualifies into C-category.

Table 2. The pavement classes of the surface state of pavement [21, 22]

Class of condition	A	B	C	D
n_m indicator values [–]	$n_m > 0.90$	$0.90 \geq n_m \geq 0.56$	$0.55 \geq n_m \geq 0.41$	$0.40 \geq n_m$
U indicator values [μm]	$U < 390$	$390 \leq U < 550$	$550 \leq U < 710$	$U \geq 710$
A – excellent condition	A new and rehabilitated surface that does not require treatment			
B – sufficient condition				
C – insufficient condition	Surfaces with distress that require planned treatment			
D – critical condition	Surfaces with distresses that require immediate actions			

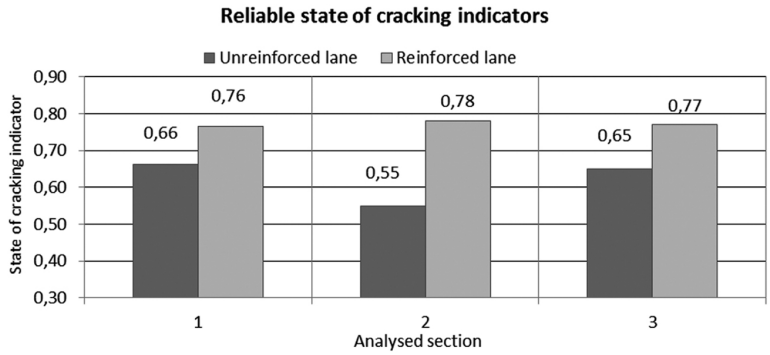

Fig. 4. A comparison of reliable cracking indicators

The indicators' values differ by an average of 0.14, and it can be presumed that the unreinforced lane will require rehabilitation treatment much earlier than the reinforced lane, as its degradation will progress faster over time; however, this assumption will be verified later with deflection measurements.

The most significant difference between reinforced and unreinforced lane can be spotted in Section 2, Section 1 and Section 3 variations are on a similar level. The lower indicator value results in a higher number of distresses produced at the surface. Every additional discontinuity in the asphalt concrete surface leads to further vulnerability to chemical and physical factors such as water penetration, freezing damage, gas, oil, and salt penetration. The next step after visual evaluation of the pavement was the deflection measurement. The threshold values of the calculated reliable deflections for this class of roads (KR3) are shown in Table 2 based on the Polish code of practice [22]. The reliable deflection is calculated from Eq. (2.5) with a confidence level of 98%, which means that the occurrence of higher deflection values is possible with a probability of 2%. This practical aspect is vital because the deflection analysis used in this paper is often used to design the asphalt concrete overlays over existing surfaces. The values of reliable deflection U are compared in the Fig. 5 for the unreinforced lane and in the Fig. 6 for the reinforced lane, divided into sections presented in Table 3. The values of us' are presented to compare the deflection standardised to the temperature of 20°C and the load of 50 kN.

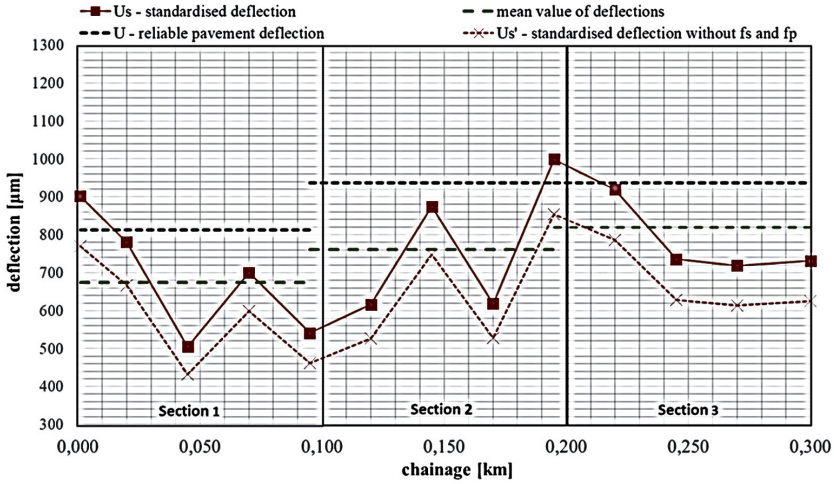

Fig. 5. Comparison of calculated deflections in the unreinforced lane for the measures taken in 2019

The most important thing to notice is that for both reinforced and unreinforced lanes, the values of reliable deflection U presented in Figs. 5 and 6 exceed the allowed deflection of 390 µm. The difference between lanes in reliable deflection values is relatively small in Sections 2 and 3 and becomes noticeable in Section 1 – 79 µm. The mean values of standardised deflections us are higher for the unreinforced lane, with the smallest difference spotted in Section 2.

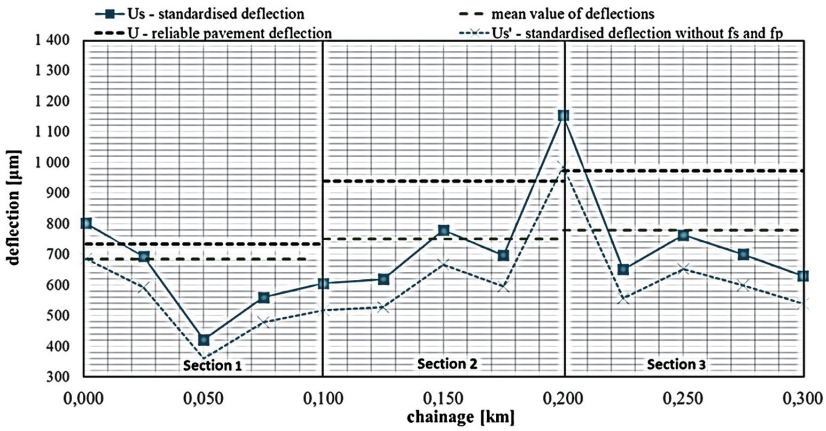

Fig. 6. Comparison of calculated deflections in the reinforced lane for the measures taken in 2019

For Section 1, the mean deflection *us* values are bigger by 9% for unreinforced lane while for Section 3, the difference between lanes is around 5%. The high values of reliable deflections may disrupt the identification of reinforcement effect because the analyzed pavement's bearing capacity is below the allowable level. Short sections of 100 m length lead to standard deviations that meaningfully impact the results for a relatively low number of measures taken. Every section of both the unreinforced and reinforced lane is classified as a critical condition (D-state in Table 2) based on reliable deflection, while the state of cracking indicator points to classes B and C. Analysis was repeated in 2021 for FWD data, the results are shown in Table 4.

The reliable deflections represent values higher than previously, indicating the pending degradation of the pavement structure as shown in Fig. 7 and 8. This analysis has shown

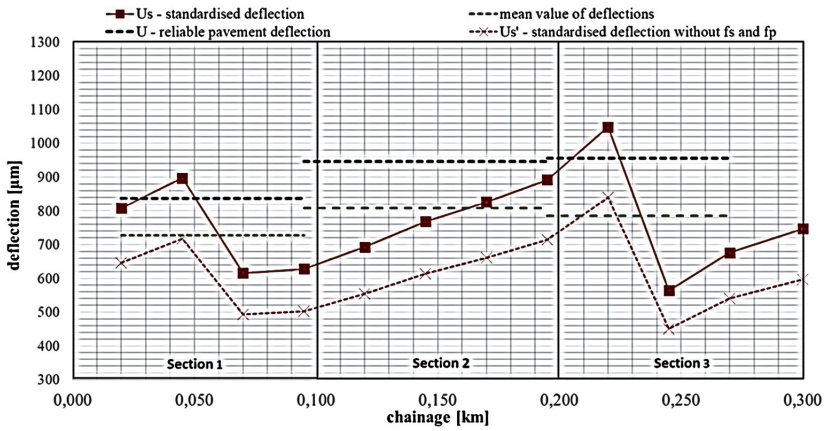

Fig. 7. Comparison of calculated deflections in the unreinforced lane for the measures taken in 2021

Table 3. Calculated values of deflections for the measures taken in 2019

Unreinforced lane					Section	Reinforced lane				
Chainage [km]	Us [μm]	Mean	Dus [μm]	U [μm]		Chainage [km]	Us [μm]	Mean	Dus [μm]	U [μm]
0.001	902	674	138	812	1	0.001	801	616	117	733
0.020	781					0.025	693			
0.045	505					0.050	421			
0.070	700					0.075	560			
0.095	541					0.100	605			
0.120	616	761	175	936	2	0.125	618	750	189	939
0.145	874					0.150	779			
0.170	618					0.175	696			
0.195	999					0.200	1153			
0.220	919	820	116	936	3	0.225	651	779	192	972
0.245	735					0.250	763			
0.270	718					0.275	700			
0.300	731					0.300	629			
Chainage [km]	Us' [μm]	Mean	Dus' [μm]	U' [μm]	Section	Chainage [km]	Us' [μm]	Mean	Dus' [μm]	U' [μm]
0.001	771	576	118	694	1	0.001	685	527	100	626
0.020	667					0.025	592			
0.045	432					0.050	360			
0.070	599					0.075	478			
0.095	462					0.100	517			
0.120	527	651	150	800	2	0.125	528	641	162	803
0.145	747					0.150	666			
0.170	528					0.175	595			
0.195	853					0.200	985			
0.220	786	701	99	800	3	0.225	556	666	165	830
0.245	629					0.250	652			
0.270	614					0.275	598			
0.300	625					0.300	538			

some differences between lanes; however, higher values were spotted in the reinforced lane. The differences range from 33 μm in Section 2 to 95 μm in Section 3. The deflection basin parameters were calculated to seek further investigation of the glass fiber mesh influence.

As shown in Fig. 9, the calculated deflection basin parameters were used to evaluate the pavement layers between reinforced and unreinforced lanes. Looking at the Base Layer

Table 4. Calculated values of deflections for the measures taken in 2021

Unreinforced lane					Section	Reinforced lane				
Chainage [km]	Us [μm]	Mean	Dus [μm]	U [μm]		Chainage [km]	Us [μm]	Mean	Dus [μm]	U [μm]
0.020	808	728	109	837	1	0.025	675	769	103	872
0.045	898					0.050	935			
0.070	616					0.075	680			
0.095	628					0.100	842			
0.120	693	809	137	946	2	0.125	714	823	156	979
0.145	768					0.150	646			
0.170	826					0.175	788			
0.195	892					0.200	806			
0.220	1049	786	169	955	3	0.225	1141	916	124	1040
0.245	564					0.250	945			
0.270	676					0.275	809			
0.300	747					0.300	879			
Chainage [km]	Us' [μm]	Mean	Dus' [μm]	U' [μm]	Section	Chainage [km]	Us' [μm]	Mean	Dus' [μm]	U' [μm]
0.020	646	583	87	670	1	0.025	540	615	82	697
0.045	718					0.050	748			
0.070	492					0.075	544			
0.095	502					0.100	673			
0.120	554	647	110	757	2	0.125	571	658	125	783
0.145	615					0.150	516			
0.170	661					0.175	631			
0.195	714					0.200	645			
0.220	839	628	135	764	3	0.225	913	733	99	832
0.245	451					0.250	756			
0.270	541					0.275	647			
0.300	598					0.300	703			

Index calculated for 2019 (Fig. 10), it may be noticed that the unreinforced lane shows higher values, which indicates that the technical condition is worse than that of the reinforced lane. Fig. 11 represents data for 2021 measurement, and confirms this observations, also showing that around km 0 + 200 weak spot of some sort is located. The Radius of Curvature values from both measures shown in Fig. 12 and 13, describing the technical condition of upper

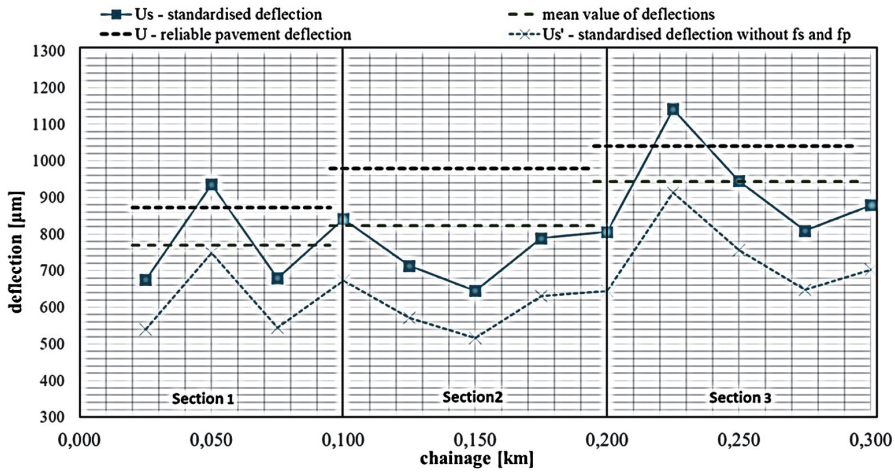

Fig. 8. Comparison of calculated deflections in the reinforced lane for the measures taken in 2021

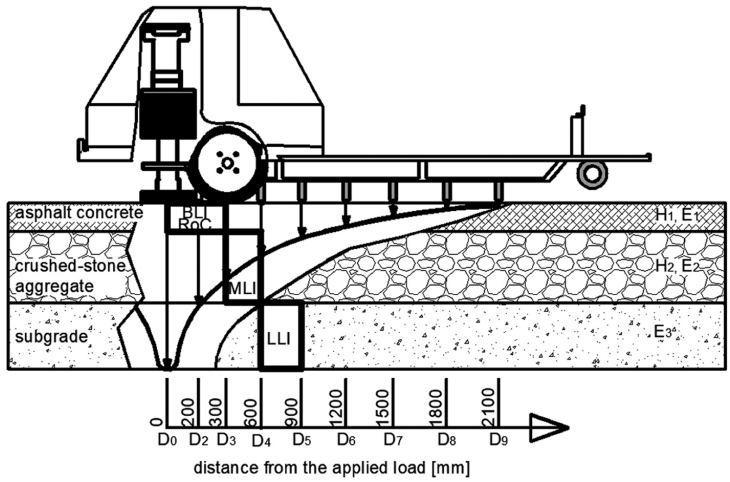

Fig. 9. Falling weight deflectometer with a bowl of deflection and curvature indices shown on a corresponding layer of pavement construction

layers of pavement are higher for reinforced lane's Sections 1 and 3 with opposite situation for lane no 2. Every section represents a good technical condition. It can be noticed that the influence of applied glass fibres mesh is seen, the values are slightly higher for a reinforced lane, whilst the BLI values differs with no visible trend. For the rest of the DBP-s, Middle Layer Index (Fig. 14 and 15) and Lower Layer Index (Figs. 16 and 17), the situation is similar and no visible influence of the applied reinforcement is seen.

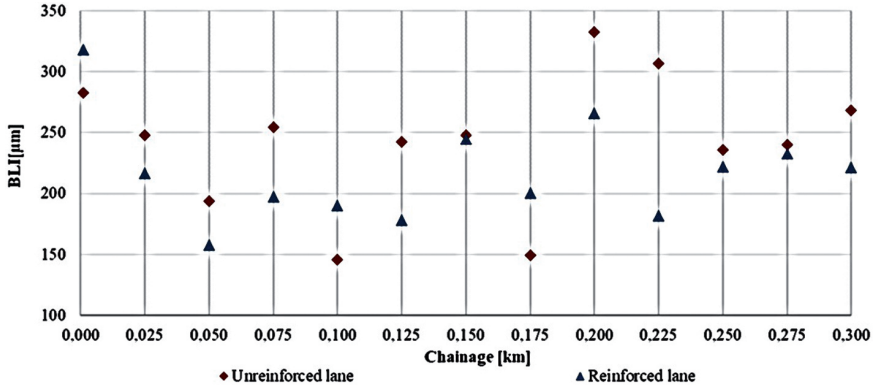

Fig. 10. Base Layer Index values for the 2019 measurement

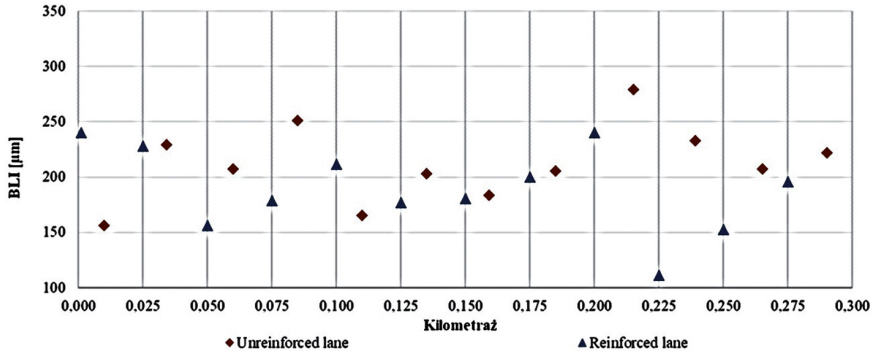

Fig. 11. Base Layer Index values for the 2019 measurement

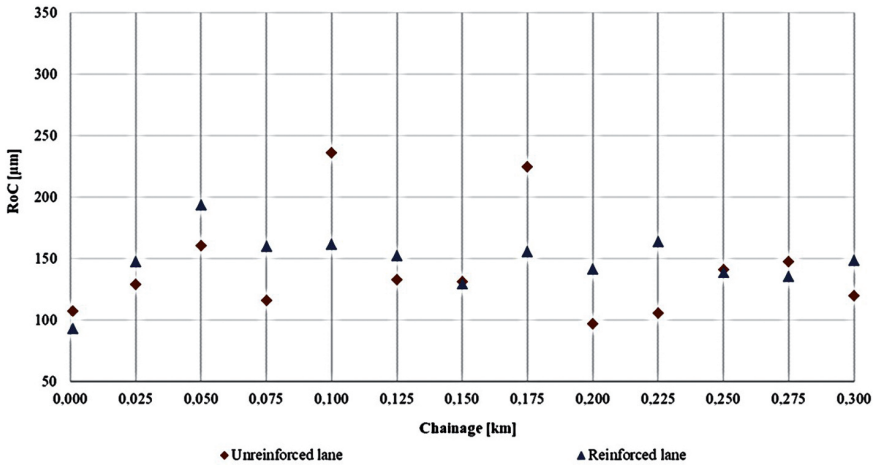

Fig. 12. Radius of Curvature values for the 2019 measurement

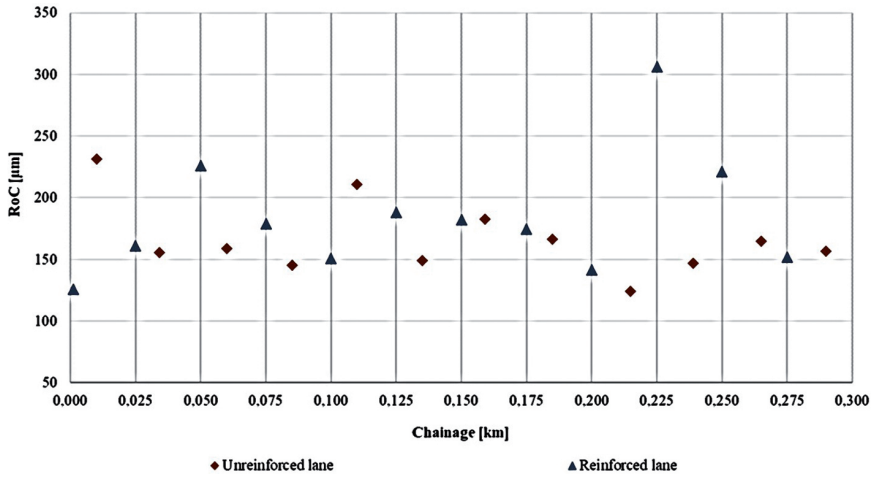

Fig. 13. Radius of Curvature values for the 2021 measurement

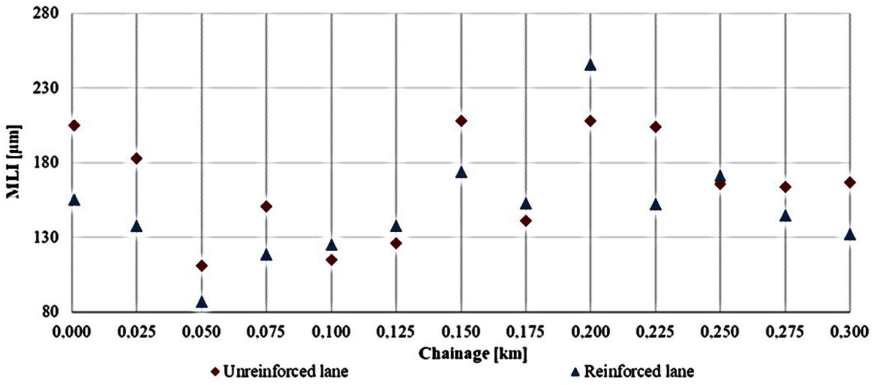

Fig. 14. Middle Layer Index values for 2019 measurement

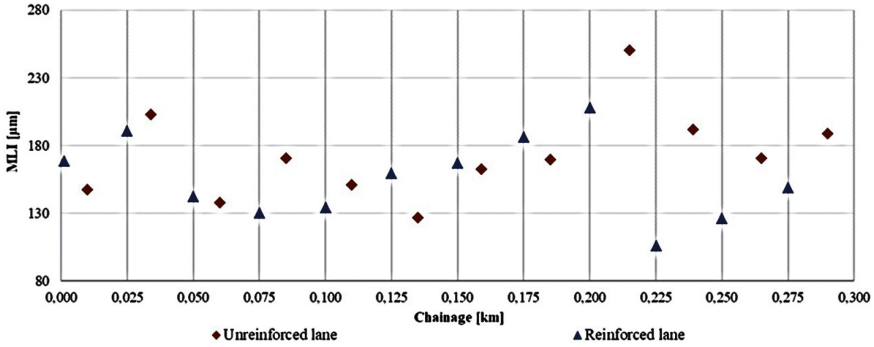

Fig. 15. Middle Layer Index values for 2021 measurement

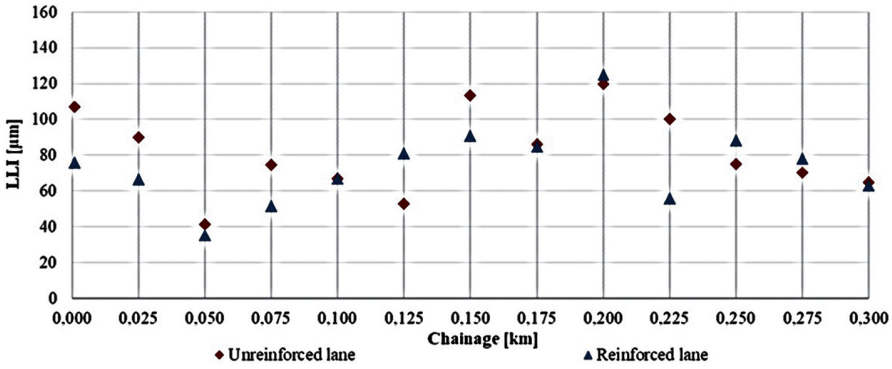

Fig. 16. Lower Layer Index values for 2019 measurement

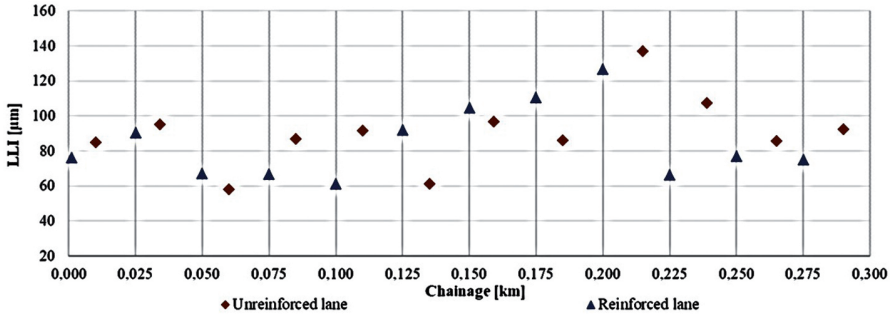

Fig. 17. Lower Layer Index values for 2021 measurement

4. Conclusions

The influence of terrain subsidence from mining excavation leads to unloosing strains in the subbase and subgrade, ultimately weakening the unbound granular layers. This negative impact on pavement construction can be obviated or prevented with the rightly designed and applied geosynthetic layers in the form of a mattress rather than a single layer divider. Analysed road, located in the area prone to terrain subsidence from mining activity, was reinforced with a single-layer of glass fibre mesh placed under asphalt concrete layers. The amount of surface distress, and by that state of cracking indicator, is significantly lower in the reinforced section of the road, and that implies the positive effects of applied reinforcement on the amount of longitudinal, transverse, and fatigue crackings. The high values of reliable deflections show that an immediate rebuild is needed. Differences between lanes are small but noticeable; however, high total values of deflections make it very difficult to determine the influence of the mesh. The data presented for deflections do not correlate with the state of cracking indicators; the values of reliable deflection points toward the critical condition (D) of pavement construction whereas the state of cracking indicator shows sufficient (B) and alarming (C) state. Additional investigation of the deflection basin parameters shows that

the applied reinforcement has a positive influence on the technical state of the asphalt layers reflected in higher values of the Radius of Curvature of the reinforcement lane. The rest of the deflection bowl parameters do not show such impact and the values differ between the lanes, usually indicating a poor technical condition of the pavement. The applied solution may prove useful in improving pavement fatigue life by reducing the number of cracks, but only for roads not located in a mining subsidence area, since no positive effect was observed on reducing the impact of terrain subsidence from mining activity. Even the lane with a reduced amount of surface distress requires immediate treatment. This may suggest that the overall pavement life in a mining subsidence area is reduced to a degree that proves any simple solutions, otherwise effective, are obsolete. It should be noted that in many cases rehabilitation treatment is used, in many cases when, in fact, the road should be rebuilt with the entire pavement construction and the following infrastructure, considering the valid traffic load and groundwater conditions. That leads to problems in designing appropriate solutions for rehabilitation treatment. It must be pointed out that for the optimisation of the proper solution, it is crucial to use the pavement structural design method that includes additional mining subsidence influence. Horizontal deformations have a major impact on pavement construction work, leading to a change of ground bearing capacity over time and producing a relative disparity in displacement between points on the surface and the ground base which activates the horizontal friction on a border between layers and causes additional tensile stress. Additional roads in different locations in mining areas of different categories need to be analysed to verify the observations made.

References

[1] M. Zięba, P. Kalisz, and M. Grygierek, "The impact of mining deformations on road pavements reinforced with geosynthetics", *Archives of Mining Sciences,* vol. 65, no. 4, pp. 751–767, 2020, doi: 10.24425/ams.2020.134145.

[2] W. Janusz, J. Zych, and M. Chudek, "Studium dotyczące stanu rozpoznania tworzenia się i prognozowania deformacji nieciągłych pod wpływem podziemnej eksploatacji złóż [Case study over genesis and prediction of non-linear surface deformation from underground deposit excavation]", *Zeszyty Naukowe Politechniki Śląskiej Seria Górnictwo*, vol. 866, no. 141, pp. 161–168, 1988.

[3] J. Kwiatek, *Obiekty budowlane na terenach górniczych [Construction objects in a mining subsidence area]*. Główny Instytut Górniczy, 2007.

[4] T. Głowacki and W. Milczarek, "Powierzchniowe deformacje wtórne dawnych terenów górniczych [Secondary surface deformations from former mining excavation]", *Mining Science*, vol. 20, pp. 39–55, 2013, doi: 10.5277/gig132004.

[5] M. Salamak, A. Radziecki, and J. Weseli, "Monitoring of highway bridges in areas under mining exploitation influence", in *5th International Conference on Current and Future Trends in Bridge Design, Construction and Maintenance, 17–18 September 2007, Beijing, China*. ICE Publishing, 2007, pp. 469–478, doi: 10.1680/bdcam.35935.0051.

[6] P. Zieliński, "Investigations of fatigue of asphalt layers with geosyntetics", *Archives of Civil Engineering,* vol. 59, no. 2, pp. 247–263, 2013, doi: 10.2478/ace-2013-0013.

[7] J. Kawalec, M. Grygierek, E. Koda, and P. Osiński, "Lessons learned on geosynthetics applications in road structures in Silesia mining region in Poland", *Applied Sciences*, vol. 9, no. 6, pp. 1–14, 2019, doi: 10.3390/app9061122.

[8] E. Pietrzyk-Sokulska, R. Uberman, and J. Kulczycka, "The impact of mining on the environment in Poland – myths and reality", *Gospodarka Surowcami Mineralnymi – Mineral Resources Management*, vol. 31, no. 1, pp. 45–64, 2015, doi: 10.1515/gospo-2015-0009.

[9] M. Borecki, *Ochrona powierzchni przed szkodami górniczymi. [Surface protection against mining activity]*. Wydawnictwo Śląsk, 1980.

[10] S. Węgliński, M. Flieger-Szymańska, M. Just, and D. Krawczyk, "Ground improvement and rebuild of a district roadin complex geotechnical-engineering conditions – case study", *Archives of Civil Engineering*, vol. 68, no. 2, pp. 63–82, 2022, doi: 10.24425/ace.2022.140630.

[11] A. Miłkowski, Z. Pilecki, K. Kłosek, and M. Tondera, "Autostrada A1 zaprojektowana na dziurawym podłożu cz. 2. [A1 highway designed in a mining area – part 2]", *Magazyn Autostrady*, no. 5, pp. 159–160, 2010.

[12] K. Kłosek, J. Sobolewski, and J. Ajdukiewicz, "Protection systems of high tensile strength geosynthetics reinforcement together with electronic permanent monitoring used in several sections of A1 Motorway situated in heavy mining active terrain in Poland", *Transportation Overview*, vol. 5, pp. 20–25, 2011.

[13] J. Kawalec, K. Chlipalski, and M. Grygierek, "Komunikacyjne obiekty liniowe na terenach górniczych. [Roads in a mining subsidence area]", *Magazyn Autostrady*, no. 3, pp. 35–42, 2015.

[14] J. Górszczyk and S. Gaca, "The influence of the carbo-glass geogrid-reinforcement on the fatigue life of the asphalt pavement structure", *Archives of Civil Engineering,* vol. 58, no. 1, pp. 97–113, 2012, doi: 10.2478/v.10169-012-0006-z.

[15] Z. Liu and H. Ling, "Performance of geosynthetic-reinforced asphalt pavements", *Journal of Geotechnical and Geoenviromental Engineering,* vol. 127, no. 2, pp. 177–184, 2001, doi: 10.1061/(ASCE)1090-0241(2001)127:2(177).

[16] H. Ling and H. Liu, "Finite element studies of asphalt concrete pavement reinforced with geogrid", *Journal of Engineering Mechanics*, vol. 129, no. 7, pp. 801–811, 2003, doi: 10.1061/(ASCE)0733-9399(2003)129:7(801).

[17] L. Nguyen, J. Blanc, J. Kerzerho, and P. Hornych, "Review of glass fibre grid use for pavement reinforcement and APT experiments at IFSTTAR", *Road Materials and Pavements Design*, vol. 14, pp. 287–308, 2013, doi: 10.1080/14680629.2013.774763.

[18] L. Jong-Hoon, B. Seung-Beom, L. Kang-Hoon, K. Jo-Soon, and J. Jin-Hoon, "Long time performance of fibre-grid-reinforced asphalt overlay pavements. A case study of Korean national highways", *Journal of Traffic and Transportation Engineering*, vol. 6, no. 4, pp. 366–382, 2019, doi: 10.1016/j.jtte.2018.01.008.

[19] I. Arsenie, C. Chazallon, J. Duchez, and P. Hornych, "Laboratory characterisation of the fatigue behaviour of glass-fibre grid-reinforced asphalt concrete using 4PB tests", *Road Materials and Pavement Design*, vol. 18, no. 1, pp. 168–180, 2017, doi: 10.1080/14680629.2016.1163280.

[20] P. Jaskuła, D. Ryś, M. Stienss, C. Szydłowski, M. Gołos, and J. Kawalec, "Fatigue performance of double-layered asphalt concrete beams reinforced with new type of geocomposites", *Materials*, vol. 14, no. 9, 2021, doi: 10.3390/ma14092190.

[21] GDDKiA, *System oceny stanu nawierzchni. Wytyczne stosowania*. Generalna Dyrekcja Dróg Krajowych i Autostrad, 2002.

[22] GDDKiA, *Diagnostyka stanu nawierzchni i wybranych elementów korpusu drogi – wytyczne stosowania*. Generalna Dyrekcja Dróg Krajowych i Autostrad, 2019.

Ocena wpływu wzmocnienia siatką z włókna szklanego na wartości parametrów krzywizny czaszy ugięć dla nawierzchni podatnej poddanej oddziaływaniom górniczym

Słowa kluczowe: tereny górnicze, siatka z włókna szklanego, osiadania terenu, FWD, parametry krzywizny czaszy ugięć

Streszczenie:

Remonty oraz przebudowy dróg zlokalizowanych na obszarach występowania oddziaływań górniczych, powinny uwzględniać efektywne oraz ekonomiczne uzasadnione rozwiązania. W analizowanym przypadku na odcinku drogi powiatowej zabudowano siatkę z włókna szklanego pod warstwami bitumicznymi, podczas remontu w 2008 roku, w taki sposób, że jeden pas drogi został wzmocniony siatką, natomiast drugi pozostawiono bez wzmocnienia. Zasadniczym celem pracy było sprawdzenie efektywności wzmocnienia w zakresie redukcji uszkodzeń nawierzchni oraz wpływ na ugięcia nawierzchni i wskaźniki krzywizny czaszy ugięć. Zaobserwowano wyraźny wpływ na obniżenie ilości spękań nawierzchni, jednak bez poprawy nośności drogi. W zakresie wskaźników krzywizny czaszy ugięć, wpływ wzmocnienia został zaobserwowany w wartościach promienia krzywizny (RoC). Stan techniczny jezdni kwalifikuje drogę do natychmiastowego remontu lub przebudowy. Zastosowane rozwiązanie nie wpłynęło wyraźnie na poprawę trwałości odcinka drogi, jednak przeprowadzone obserwacje stanowią interesujący wstęp do dalszych badań.

Received: 2022-10-12, Revised: 2023-03-14